

Parametric Sparse Bayesian Dictionary Learning for Multiple Sources Localization with Propagation Parameters Uncertainty and Nonuniform Noise

Kangyong You, *Student Member, IEEE*, Wenbin Guo, *Member, IEEE*,
Tao Peng, Yueliang Liu, Peiliang Zuo, and Wenbo Wang, *Senior Member, IEEE*

Abstract—Received signal strength (RSS) based source localization method is popular due to its simplicity and low cost. However, this method is highly dependent on the propagation model which is not easy to be captured in practice. Moreover, most existing works only consider the single source and the identical measurement noise scenario, while in practice multiple co-channel sources may transmit simultaneously, and the measurement noise tends to be nonuniform. In this paper, we study the multiple co-channel sources localization (MSL) problem under unknown nonuniform noise, while jointly estimating the parametric propagation model. Specifically, we model the MSL problem as being parameterized by the unknown source locations and propagation parameters, and then reformulate it as a joint parametric sparsifying dictionary learning (PSDL) and sparse signal recovery (SSR) problem which is solved under the framework of sparse Bayesian learning with iterative parametric dictionary approximation. Furthermore, multiple snapshot measurements are utilized to improve the localization accuracy, and the Cramér-Rao lower bound (CRLB) is derived to analyze the theoretical estimation error bound. Comparing with the state-of-the-art sparsity-based MSL algorithms as well as CRLB, extensive simulations show the importance of jointly inferring the propagation parameters, and highlight the effectiveness and superiority of the proposed method.

Index Terms—Multiple sources localization, unknown propagation parameters, sparse Bayesian learning, parametric dictionary approximation.

I. INTRODUCTION

LOCALIZATION has been attracting attention in many applications, across from commercial, industrial to defense areas, such as wireless networks, cognitive radio networks, spectrum monitoring, wireless sensor networks (WSNs), radar, and sonar [1]. In particular, source localization in WSNs has far-reaching applications [2], [3], where WSNs consist of a large number of cheap, densely deployed sensors with limited sensing and communication abilities, which monitor a spatial

physical phenomenon (e.g. temperature, sound intensity, radio signal intensity, pollution concentrations, etc.) and regularly report their measurements to a Fusion Center (FC).

According to the information available for localization in time domain, frequency domain, angular domain, and energy domain, several representative source localization methods have been proposed over the past years, such as time of arrival (TOA) [4], time difference of arrival (TDOA) [5], frequency difference of arrival (FDOA) [6], direction of arrival (DOA) [7], [8] and RSS based localization algorithms [9]–[13]. In these methods, sophisticated ones are often with high accuracy but pay the price of advanced radio receiver, processing, and communication abilities, e.g., DOA approach for narrowband signal sources requires multiple antennas or antenna array, while TOA, TDOA, or FDOA for wideband signal sources face the challenges of timing synchronization, coherent demodulation, and high-speed analog-to-digital conversion (ADC) (especially when ultra-wideband signal are interested [14]). Besides, DOA, TOA, TDOA, and FDOA are very sensitive to the availability of line of sight (LOS). On the contrary, RSS measurements, operating in both LOS and non-LOS (NLOS) environments and readily available from any radio interface, are simple and require no additional sensor functionalities. As a result, RSS-based source localization approaches have gained popularity in WSNs where simplicity, low energy consumption and low cost are the main requirements.

A. Related Works

In the past decades, many RSS-based source localization approaches have been proposed (see the overviews in [1], [15], [16]). Early literature devotes to single source localization (SSL). In the early ages of RSS-based SSL, range-based localization was achieved through trilateration [17] or multilateration algorithms [18]. These techniques are simple but suboptimal, and their accuracy is also limited. The maximum likelihood estimate (MLE) based approaches [19], [20] are more accurate but highly nonlinear, nonconvex and exhausted to search for the global maximum. Recently, there has been an increasing interest in relaxing the MLE problem, such as algorithms based on the linear least squares (LLS) [21], [22], the projection onto convex sets [23] and the semidefinite programming (SDP) [24].

Later, more and more efforts are focusing on MSL where energy information of multiple co-channel sources are coupled in RSS measurement since they share the same time and frequency resources. This phenomenon exists extensively in many applications, such as acoustic sources localization where multiple sources may make sounds simultaneously, spectrum

Manuscript received Month Day, Year; revised Month Day, Year; accepted Month Day, Year. Date of publication Month Day, Year; date of current version Month Day, Year. This work was supported by the National Natural Science Foundation of China (61271181, 61571054), the Science and Technology on Information Transmission and Dissemination in Communication Networks Laboratory Foundation. The associate editor coordinating the review of this manuscript and approving it for publication was Editor. (*Corresponding author: Wenbin Guo.*)

K. You and W. Guo are with the School of Information and Communication Engineering, Beijing University of Posts and Telecommunications, Beijing 100876, China, and also with the Science and Technology on Information Transmission and Dissemination in Communication Networks Laboratory, Shijiazhuang 050000, China (e-mail: {ykyiwiang, gwb}@bupt.edu.cn).

T. Peng, Y. Liu, P. Zuo and W. Wang are with the School of Information and Communication Engineering, Beijing University of Posts and Telecommunications, Beijing 100876, China (email: {pengtao, liuyueliang, zplzpl88, wbwang}@bupt.edu.cn).

monitoring where an illegal radio occupies the legal user's frequency band, cognitive radio where primary users and secondary users share the same time and frequency resources. Moreover, with the rapid advancement of 5G communication, non-orthogonal multiple access (NOMA) techniques and 5G enabled Internet-of-things (IoT) applications [25] will make this phenomenon more ubiquitous. In the multiple co-channel sources scenario, localization problem turns tougher and more challenging, while the aforementioned SSL methods fail to make it.

To locate multiple sources, the region of interest (ROI) is usually discretized into a set of grid points (GPs) as searching space (or location candidates). MLE approach was first proposed in [11] where a combination of multiresolution search algorithm and expectation-maximum (EM)-like algorithm was used to perform exhausted coordinate search along each dimension in searching space. Later, to reduce the computation cost, and to improve the estimation performance as well as robustness in the presence of noise and small observation size, spatial sparsity based approaches have been gradually gaining popularity [26]–[30]. The main idea is that assume sources are located on the predefined GPs, and then under specific conditions [31], multiple source locations can be estimated by searching the sparsest solution of an underdetermined linear localization equation [27]. Nevertheless, sources may deviate from the predefined GPs (off-grid) in reality, which will impair the localization performance greatly. In compressive sensing (CS) theory [31], off-grid sources bring basis mismatch problem which can not be eliminated by finer grid granularity [32]. Recently, some methods have been proposed to address the off-grid sources localization problem [33]–[35].

However, a major challenge for RSS-based localization lies in the uncertainty of propagation model. All of aforementioned works assume the characteristics of the propagation model are known and given. Nevertheless, the propagation model in practical application is not easy to be captured with time-varying propagation environment. Generally, the propagation process is characterized by some propagation parameters, such as the path-loss exponent (PLE) and transmitted powers. The single source localization problem with unknown propagation parameters has been addressed in [36]–[39]. In [36], a linear regression model was proposed for PLE estimate, and the total least squares (TLS) method was exploited to infer the unknown PLE. In [37], a Bayesian minimum mean square error (MMSE) estimator was developed to locate the source with unknown PLE. In [38], semidefinite programming (SDP) relaxation technique was adopted to estimate the transmitted power of the source. In [39], the source was located with unknown PLE and unknown transmitted powers through solving a general trust region problem. Nevertheless, the MSL problem has not been well addressed with unknown propagation parameters.

B. Contributions

In this paper, we extend the RSS-based SSL work of [39] to locate multiple co-channel sources in the presence of uncertain path-loss exponent and unknown transmitted powers. Moreover, we consider the more general case of nonuniform measurement noise and multiple snapshots model. To this end,

an efficient parametric sparse Bayesian dictionary learning (PSBDL) algorithm is proposed. The main contributions of this paper are summarized as follows.

- 1) To the best of our knowledge, we first provide a unified framework to locate multiple sources while jointly inferring the propagation parameters utilizing spatial sparsity. Specifically, we provide a localization model parameterized by source locations and propagation parameters. Then, we propose an approximation model to learn the sparsifying parameterized localization dictionary.
- 2) Under the proposed localization model, we reformulate the MSL problem as a joint PSDL and SSR problem which is effectively solved by incorporating the proposed parametric dictionary approximation model with multiple measurement vector (MMV) sparse Bayesian learning framework.
- 3) We provide CRLB analysis for the considered problem, and compare the proposed method with the state-of-the-art spatial sparsity based MSL methods. Extensive simulations show the importance of jointly estimating the propagation parameters, and highlight the effectiveness of the proposed framework.

The remainder of this paper is organized as follows: Section II first presents the proposed localization dictionary model and parameterized dictionary approximation model, and then reformulate the MSL problem. Section III is devoted to developing the proposed PSBDL algorithm. Section IV elaborates on the derivation of the CRLB. Numerical simulation results are reported in Section V. Discussion is presented in Section VI. Section VII closes this paper with conclusions.

Notation: x_i is the i -th entry of a vector \mathbf{x} . \mathbf{A}_i , \mathbf{A}^i , and $A_{i,j}$ are the i -th column, i -th row, and (i,j) -th entry of a matrix \mathbf{A} . $\|\cdot\|_0$, $\|\cdot\|_1$, $\|\cdot\|_2$, and $\|\cdot\|_F$ denote the pseudo- ℓ_0 norm, ℓ_1 norm, ℓ_2 norm, and Frobenius norm, respectively. $(\cdot)^T$ denotes transpose operator. $\text{tr}(\cdot)$ and $|\cdot|$ denote the trace and determinant operator, respectively. $\text{diag}(\mathbf{x})$ is a diagonal matrix with vector \mathbf{x} being its diagonal elements. $\text{diag}(\mathbf{A})$ denotes a column vector composed with the diagonal elements of matrix \mathbf{A} . \circ is the Hadamard (element-wise) product operator. For clear and concise presentation, some functions are abbreviated sometimes by omitting the input variables in context, e.g. $\Phi(\theta)$ is abbreviated as Φ , and $f(s_i, t_k, \gamma)$ abbreviated as f . $\mathbf{1}_N$ and \mathbf{I}_N denote the all ones vector and the identity matrix of dimension N , respectively.

II. PROBLEM FORMULATION

In this section, we first revisit the fundamentals of sparsity-based MSL problem, and present the proposed localization model considering both the unknown source locations and the unknown propagation parameters. Then, we proposed a parameterized dictionary approximation model and reformulate the MSL problem as a joint PSDL and SSR problem.

A. MSL Model

The system of consideration consists of K sources with unknown locations $\mathcal{T} = \{\mathbf{t}_k = [\mathbf{u}_k^T, \mathbf{v}_k^T]^T, k = 1, \dots, K\}$ and M passive sensors with known locations $\mathcal{S} = \{\mathbf{s}_i = [\mathbf{u}_i^S, \mathbf{v}_i^S]^T, i = 1, \dots, M\}$ in

a two-dimensional ROI with u and v being the Cartesian coordinates. The RSS measurement of the i -th sensor at time snapshot t can be expressed as [11]

$$y_i(t) = \sum_{k=1}^K P_k(t) f(s_i, t_k, \gamma) + \varepsilon_i(t), \quad (1)$$

where $\varepsilon_i(t)$, $f(\cdot)$, $P_k(t)$, and γ are the unknown measurement noise of sensor i at time t , the propagation model, the transmitted power of source k at a reference distance d_0 at time t , and the PLE, respectively. Generally, the PLE varies from 2 (free space) to 6 (e.g., some indoor scenario) [39], and is off-line calibrated in conventional routine. The matrix-vector formulation of the single measurement vector (SMV) signal model for time t is:

$$\mathbf{y}(t) = \Phi(\mathcal{T}, \gamma) \boldsymbol{\omega}(t) + \boldsymbol{\epsilon}(t), \quad (2)$$

with $\boldsymbol{\epsilon}(t) = [\varepsilon_1(t), \dots, \varepsilon_M(t)]^T$, $\mathbf{y}(t) = [y_1(t), \dots, y_M(t)]^T$, $\boldsymbol{\omega}(t) = [P_1(t), \dots, P_K(t)]^T$, $\Phi(\mathcal{T}, \gamma)_{i,k} = f(s_i, t_k, \gamma)$.

We further consider there are T snapshots RSS measurement available, denote $\mathbf{Y} = [\mathbf{y}(1), \dots, \mathbf{y}(T)]$, $\mathbf{W} = [\boldsymbol{\omega}(1), \dots, \boldsymbol{\omega}(T)]$ and $\mathbf{E} = [\boldsymbol{\epsilon}(1), \dots, \boldsymbol{\epsilon}(T)]$, and then the SMV model in (2) evolves into the MMV model as

$$\mathbf{Y} = \Phi(\mathcal{T}, \gamma) \mathbf{W} + \mathbf{E}, \quad (3)$$

with $\mathbf{Y}, \mathbf{E} \in \mathbb{R}^{M \times T}$, $\mathbf{W} \in \mathbb{R}^{K \times T}$, and $\Phi(\mathcal{T}, \gamma) \in \mathbb{R}^{M \times K}$. Thus, the SMV signal model in (1) is a special case when $T = 1$.

Generally, the noise statistics of the sensors observations are different. Thus, we assume $\boldsymbol{\epsilon}(t)$ is a nonuniform noise. As a result, the MSL task can be summarized as given the measurement matrix \mathbf{Y} , sensor location set \mathcal{S} , and parametric propagation model $f(s_i, t_k, \gamma)$, how to infer the source location set \mathcal{T} in the presence of unknown nonuniform noise \mathbf{E} and unknown propagation parameters γ and P_k , for $k = 1, \dots, K$.

B. Traditional Spatial Sparsity Based MSL Methods

To alleviate the problem difficulty, traditional sparsity-based methods ([26]–[30], etc.) assume that the PLE is precisely known, and all sources are located on predetermined candidate GP set $\mathcal{G} = \{\mathbf{g}_j = [u_j, v_j], j = 1, \dots, N\}$, i.e. $\mathcal{T} \subset \mathcal{G}$.

Assume the sources are static during the observation period, then \mathbf{Y} has sparse representation in a localization dictionary $\Phi(\mathcal{G})$ with the fact that $K \ll N$. Therefore, the MSL model in (3) can be cast into a standard sparse recovery model as

$$\mathbf{Y} = \Phi(\mathcal{G}) \mathbf{X} + \mathbf{E}, \quad (4)$$

where $\mathbf{X} = [\mathbf{x}(1), \dots, \mathbf{x}(T)]$ and $\mathbf{X}_{i,t} = P_k(t)$ when source k locates on GP i , and otherwise $\mathbf{X}_{i,t} = 0$. Thus \mathbf{X} is a common sparse (or row-sparse) coefficient matrix [40], i.e., all the columns \mathbf{X}_t share the same sparse support. As a result, the row support of \mathbf{X} encodes the source locations in candidate GP set \mathcal{G} and the corresponding rows in \mathbf{X} encode the transmitted powers in different time snapshots.

In this way, localization can be transformed into a standard MMV row-sparse recovery problem as

$$\hat{\mathbf{X}} = \arg \min_{\mathbf{X}} \mathcal{R}(\mathbf{X}), \text{ s.t. } \|\mathbf{Y} - \Phi(\mathcal{G}) \mathbf{X}\|_F < \epsilon, \quad (5)$$

where ϵ bounds the amount of noise in \mathbf{Y} , and $\mathcal{R}(\mathbf{X})$ denotes the row sparsity of \mathbf{X} , i.e., the number of non-zero rows.

Problem (5) can be solved using standard MMV compressive sensing methods, such as S-OMP [41], M-BP [42], M-FOCCUS [43], M-SBL [44], etc. In particular, details about traditional sparsity-based MSL when $T = 1$ are referred to [26]–[30].

C. The Proposed Parametric Dictionary Model and Its Approximation

In practice, source locations may deviate from the predefined candidate GPs and the off-line calibrated path-loss exponent may differ from that in on-line RSS measurement. Thus, it is more realistic and important to treat the candidate GP set \mathcal{G} and the PLE γ as unknown variables to be inferred from the on-line RSS measurements. To this end, the localization dictionary is modeled as $\Phi(\mathcal{G}, \gamma)$. Accordingly, the MSL model (4) evolves into

$$\mathbf{Y} = \Phi(\mathcal{G}, \gamma) \mathbf{X} + \mathbf{E}, \quad (6)$$

and the corresponding optimization problem turns into the following joint PSDL and SSR problem

$$(\hat{\mathbf{X}}, \hat{\Phi}) = \arg \min_{\mathbf{X}, \Phi} \mathcal{R}(\mathbf{X}) \quad (7a)$$

$$\text{s.t. } \|\mathbf{Y} - \Phi(\mathcal{G}, \gamma) \mathbf{X}\|_F < \epsilon, \quad (7b)$$

However, to infer $\Phi(\mathcal{G}, \gamma)$ directly is nearly impossible since the goal function w.r.t. the dictionary parameters \mathcal{G} and γ is highly nonconvex. As a result, some approximation methods must be resorted to. Have in mind that in the implementation of an iterative algorithm, the dictionary parameters are often initialized with $\mathcal{G}^{(0)}$ and $\gamma^{(0)}$ to construct an initial dictionary which will be updated in the subsequent inference. Thus, denote by $\bar{\mathcal{G}}$ the proper candidate GP set satisfying $\mathcal{T} \subset \bar{\mathcal{G}}$, $\bar{\gamma}$ the true PLE, $\delta_g = [\delta_u, \delta_v]$ the grid offset to $\bar{\mathcal{G}}$ of the current grid estimation $\mathcal{G}^{(k)}$, δ_γ the PLE offset to $\bar{\gamma}$ of the current PLE estimation $\gamma^{(k)}$, we can expand the dictionary by each entry using Taylor series, and approximate it through keeping the linear parts as

$$\begin{aligned} \Phi(\bar{\mathcal{G}}, \bar{\gamma}) &\approx \Phi_0 + \Phi'_u(\mathcal{G}^{(k)}, \gamma^{(k)}) \text{diag}(\delta_u) \\ &+ \Phi'_v(\mathcal{G}^{(k)}, \gamma^{(k)}) \text{diag}(\delta_v) + \delta_\gamma \Phi'_\gamma(\mathcal{G}^{(k)}, \gamma^{(k)}) \end{aligned} \quad (8)$$

where $\Phi_0 = \Phi(\mathcal{G}^{(k)}, \gamma^{(k)})$ and for $\chi = u, v, \gamma$, Φ'_χ is the partial differential matrix with the (i, j) -th entry being the partial differential item expressed as $(\Phi'_\chi)_{i,j} = \partial f(s_i, \mathbf{g}_j, \gamma) / \partial \chi$.

D. Problem Reformulation

Based on above approximation model, we can relax and solve the joint optimization problem (7) iteratively. In each iteration, given current dictionary parameter as $\mathcal{G}^{(k)}$, $\gamma^{(k)}$, we

have to settle the following joint PSDL and SSR subproblem

$$\left(\hat{\mathbf{X}}, \hat{\delta}_g, \hat{\delta}_\gamma\right) = \arg \min_{\mathbf{X}, \delta_g, \delta_\gamma} \mathcal{R}(\mathbf{X}) \quad (9a)$$

s.t.

$$\Phi_0 = \Phi\left(\mathcal{G}^{(k)}, \gamma^{(k)}\right), \quad (9b)$$

$$\begin{aligned} \Phi = \Phi_0 + \Phi'_u\left(\mathcal{G}^{(k)}, \gamma^{(k)}\right) \text{diag}(\delta_u) + \delta_\gamma \Phi'_\gamma\left(\mathcal{G}^{(k)}, \gamma^{(k)}\right) \\ + \Phi'_v\left(\mathcal{G}^{(k)}, \gamma^{(k)}\right) \text{diag}(\delta_v), \end{aligned} \quad (9c)$$

$$\|\mathbf{Y} - \Phi\mathbf{X}\|_F < \epsilon, \quad (9d)$$

$$\delta_u \in [LB_u, UB_u], \delta_v \in [LB_v, UB_v], \delta_\gamma \in [LB_\gamma, UB_\gamma] \quad (9e)$$

with LB_χ, UB_χ being the lower and upper boundary for $\delta_\chi, \chi = u, v, \gamma$, respectively.

Once problem (9) is solved, we can update the dictionary parameters simply as

$$\mathcal{G}^{(k+1)} = \mathcal{G}^{(k)} + \hat{\delta}_g, \quad \gamma^{(k+1)} = \gamma^{(k)} + \hat{\delta}_\gamma, \quad (10)$$

and then solve the subproblem again until it converges.

III. PARAMETRIC SPARSE BAYESIAN DICTIONARY LEARNING FOR MULTIPLE SOURCES LOCALIZATION

In this section, we are devoted to solving problem (9) from the perspective of probabilistic inference. First, a hierarchical sparsity-promoting probabilistic model is imposed for model (6). Then, problem (9) is solved based on Bayesian inference. At last, the proposed PSBDL algorithm is summarized, and its complexity is discussed.

A. Hierarchical Sparse Probabilistic Model

The hierarchical probabilistic model is expressed as

$$\mathbf{E} | \beta \sim \prod_{t=1}^T \mathcal{N}(\varepsilon(t) | 0, \text{diag}(\beta)^{-1}), \quad (11a)$$

$$\beta; a, b \sim \prod_{j=1}^M \text{Gamma}(\beta_j | a, b), \quad (11b)$$

$$\mathbf{X} | \alpha \sim \prod_{t=1}^T \mathcal{N}(\mathbf{x}(t) | 0, \text{diag}(\alpha)), \quad (11c)$$

$$\alpha; \lambda \sim \prod_{i=1}^N \text{Gamma}\left(\alpha_i | 1, \frac{\lambda}{2}\right), \quad (11d)$$

$$\gamma \sim \text{Uniform}(\gamma | 2, 6), \quad (11e)$$

where the probability density function (PDF) of a multivariate Gaussian distribution random variable \mathbf{x} with mean $\boldsymbol{\mu}$ and covariance $\boldsymbol{\Sigma}$ is

$$\mathcal{N}(\mathbf{x} | \boldsymbol{\mu}, \boldsymbol{\Sigma}) = \frac{1}{\sqrt{(2\pi)^N |\boldsymbol{\Sigma}|}} \exp\left\{-\frac{(\mathbf{x} - \boldsymbol{\mu})^T \boldsymbol{\Sigma}^{-1} (\mathbf{x} - \boldsymbol{\mu})}{2}\right\}, \quad (12)$$

the PDF of a Gamma distribution random variable x with shape parameter a and rate parameter b is

$$\text{Gamma}(x; a, b) = \Gamma(a)^{-1} b^a x^{a-1} \exp\{-bx\} \quad (13)$$

with $\Gamma(\cdot)$ being the Gamma function, the PDF of a uniform distribution random variable x in the interval of $[a, b]$ is

$$\text{Uniform}(x; a, b) = \frac{1}{b-a}. \quad (14)$$

Intuitively, for $t = 1, \dots, T$, noise $\varepsilon(t)$ is independent identically distributed (i.i.d.) nonuniform Gaussian random variables

whose variance is governed by the conjugate hyperprior shown in (11b). Moreover, all columns of \mathbf{X} are independent and share the same prior which is shown in [45] to be a Laplace distribution as

$$\begin{aligned} p(\mathbf{x}(t); \lambda) &= \int p(\mathbf{x}(t) | \alpha) p(\alpha; \lambda) d\alpha \\ &= \frac{\sqrt{\lambda}}{2} \exp\left\{-\sqrt{\lambda} \|\mathbf{x}(t)\|_1\right\}. \end{aligned} \quad (15)$$

Above Laplace distribution is also termed as Bayesian LASSO [46] whose counterpart in optimization theory, LASSO, is the best convex approximation to the ℓ_0 -norm. The distribution in (15) is strongly peaked at the origin, thus it is a sparse prior that favors most entries of vector $\mathbf{x}(t)$ being zeros. Since all columns of \mathbf{X} are governed by the same sparse prior, the two-stage hierarchical prior shown in (11c) and (11d) is a row-sparsity promoting prior which favors most rows of \mathbf{X} being zeros.

According to the above hierarchical probabilistic modeling, we have the joint PDF as

$$p(\mathbf{X}, \mathbf{Y}, \alpha, \beta, \gamma; \mathcal{G}) = p(\mathbf{Y} | \mathbf{X}, \beta, \gamma; \mathcal{G}) p(\mathbf{X} | \alpha) p(\alpha) p(\beta) p(\gamma). \quad (16)$$

B. Sparse Bayesian Inference

Combining the approximation model in subsection (II-C) and the sparse probabilistic model in (III-A), we are able to address the joint optimization subproblem (9) by Bayesian inference. In the following, $\Phi(\mathcal{G}, \gamma)$ is abbreviated as Φ for simplicity, and we denote $\mathbf{A} = \text{diag}(\alpha)$, $\mathbf{B} = \text{diag}(\beta)$. Bayesian inference starts with the full posterior probability $p(\mathbf{X}, \alpha, \beta, \gamma | \mathbf{Y}; \mathcal{G})$ which can be decomposed as

$$p(\mathbf{X}, \alpha, \beta, \gamma | \mathbf{Y}; \mathcal{G}) = p(\mathbf{X} | \mathbf{Y}, \alpha, \beta, \gamma; \mathcal{G}) p(\alpha, \beta, \gamma | \mathbf{Y}; \mathcal{G}). \quad (17)$$

It is shown that the posterior distribution of \mathbf{X} is Gaussian [45]

$$\begin{aligned} p(\mathbf{X} | \mathbf{Y}, \alpha, \beta, \gamma; \mathcal{G}) &= \frac{p(\mathbf{Y} | \mathbf{X}, \beta, \gamma; \mathcal{G}) p(\mathbf{X} | \alpha)}{p(\mathbf{Y} | \alpha, \beta, \gamma; \mathcal{G})} \\ &= \prod_{t=1}^T \mathcal{N}(\mathbf{x}(t) | \boldsymbol{\mu}(t), \boldsymbol{\Sigma}), \end{aligned} \quad (18)$$

with

$$\boldsymbol{\Sigma} = \left(\Phi^T \mathbf{B} \Phi + \mathbf{A}^{-1}\right)^{-1}, \quad (19)$$

$$\boldsymbol{\mu}(t) = \boldsymbol{\Sigma} \Phi^T \mathbf{B} \mathbf{y}(t). \quad (20)$$

To calculate $\boldsymbol{\Sigma}$ and $\boldsymbol{\mu}(t)$, we need to estimate the dictionary parameter \mathcal{G}, γ and probabilistic model hyperparameters α, β . Similar to [40], [45], [47], [48], type-II maximum likelihood procedure is utilized, thus $\alpha, \beta, \mathcal{G}$, and γ are approximated by its maximum a posteriori probability estimation (MAP).

$$(\alpha, \beta, \mathcal{G}, \gamma) = \arg \max_{\alpha, \beta, \mathcal{G}, \gamma} p(\alpha, \beta, \gamma | \mathbf{Y}; \mathcal{G}) \quad (21a)$$

$$= \arg \max_{\alpha, \beta, \mathcal{G}, \gamma} p(\mathbf{Y}, \alpha, \beta, \gamma; \mathcal{G}) \quad (21b)$$

$$= \arg \max_{\alpha, \beta, \mathcal{G}, \gamma} \ln p(\mathbf{Y}, \alpha, \beta, \gamma; \mathcal{G}). \quad (21c)$$

In (21c), maximizing the logarithmic marginal likelihood $\ln p(\mathbf{Y}, \alpha, \beta, \gamma; \mathcal{G})$ by finding the stationary point is feasible

but lacking guaranteed performance since the goal function $\ln p(\mathbf{Y}, \alpha, \beta, \gamma; \mathcal{G})$ is multimodal and nonconvex. Instead, we use the expectation maximization (EM) method to iteratively maximize its evidence lower bound (ELBO) $E \{\ln p(\alpha, \beta, \mathbf{Y}, \mathbf{X}, \gamma; \mathcal{G})\}$ by treating \mathbf{X} as hidden variables, where $E \{\cdot\}$ denotes an expectation w.r.t. the posterior of \mathbf{X} given in (18). As a result, we have the following update rules.

1) *EM Update for Probabilistic Model Parameter β and α :* To maximize the ELBO w.r.t β and α is equivalent to maximize $E \{\ln p(\mathbf{X}|\alpha)p(\alpha)\}$ and $E \{p(\mathbf{Y}|\mathbf{X}, \beta, \gamma; \mathcal{G})p(\beta)\}$ respectively, which leads to the following update rules

$$\alpha_i^{\text{new}} = \frac{\sqrt{T^2 + 4\lambda \sum_{t=1}^T (\Sigma_{ii} + \mu(t)_i^2)} - T}{2\lambda}, \text{ for } i = 1, \dots, N, \quad (22)$$

$$\beta_j^{\text{new}} = \frac{2a - 2 + T}{2b + \sum_{t=1}^T (\text{Res}(t)_j^2 + \Delta_{jj})}, \text{ for } j = 1, \dots, M, \quad (23)$$

with $\mathbf{Res}(t) = \mathbf{y}(t) - \Phi\mu(t)$, $\mathbf{\Lambda} = \Phi\Sigma\Phi^T$. For simplicity expression, the derivations of (22) and (23) are presented in Appendix A and Appendix B, respectively.

2) *EM Update for Dictionary Model Parameter \mathcal{G} and γ :* The localization dictionary is parametrized by \mathcal{G} and γ , thus to learn the sparsifying localization dictionary is equal to learn the corresponding dictionary parameters. According to (16), the maximization of the ELBO w.r.t. to \mathcal{G} and γ is equivalent to maximize $E \{\ln p(\mathbf{Y}|\mathbf{X}, \beta, \gamma; \mathcal{G})p(\gamma)\}$ which is tantamount to minimize

$$E \left\{ \sum_{t=1}^T (\mathbf{y}(t) - \Phi\mathbf{x}(t))^T \mathbf{B} (\mathbf{y}(t) - \Phi\mathbf{x}(t)) \right\} \\ = \sum_{t=1}^T \left\{ (\mathbf{y}(t) - \Phi\mu(t))^T \mathbf{B} (\mathbf{y}(t) - \Phi\mu(t)) + \text{tr} (\Phi\Sigma\Phi^T \mathbf{B}) \right\}. \quad (24)$$

By incorporating the dictionary approximation model (9b),(9c) into above goal function, minimizing (24) boils down to solving the following linear least square (LLSQ) problem with boundary constraints as

$$\arg \min_{\delta_u, \delta_v, \delta_\gamma} \left\{ \begin{array}{l} \delta_u^T M_{uu} \delta_u + \delta_v^T M_{vv} \delta_v + p\delta_\gamma^2 + 2\delta_u^T M_{uv} \delta_v \\ + 2\delta_\gamma v_{u\gamma}^T \delta_u + 2\delta_\gamma v_{v\gamma}^T \delta_v + 2v_u^T \delta_u + 2v_v^T \delta_v + 2q\delta_\gamma \end{array} \right\} \quad (25a)$$

$$\text{s.t. } \delta_u \in [LB_u, UB_u], \delta_v \in [LB_v, UB_v], \delta_\gamma \in [LB_\gamma, UB_\gamma]. \quad (25b)$$

with

$$M_{uu} = \Phi_u'^T \mathbf{B} \Phi_u', \quad (26a)$$

$$M_{vv} = \Phi_v'^T \mathbf{B} \Phi_v', \quad (26b)$$

$$M_{uv} = \Phi_u'^T \mathbf{B} \Phi_v', \quad (26c)$$

$$v_{u\gamma} = \left[\Phi_u'^T \mathbf{B} \Phi_\gamma' \circ (T \cdot \Sigma + UU^T) \right] \cdot \mathbf{1}_N, \quad (26d)$$

$$v_{v\gamma} = \left[\Phi_v'^T \mathbf{B} \Phi_\gamma' \circ (T \cdot \Sigma + UU^T) \right] \cdot \mathbf{1}_N, \quad (26e)$$

$$v_u = T \cdot \text{diag} (\Phi_u'^T \mathbf{B} \Phi_0 \Sigma) - \sum_{t=1}^T \text{diag} (\mu(t)) \Phi_u'^T \mathbf{B} (\mathbf{y}(t) - \Phi_0 \mu(t)), \quad (26f)$$

$$v_v = T \cdot \text{diag} (\Phi_v'^T \mathbf{B} \Phi_0 \Sigma) - \sum_{t=1}^T \text{diag} (\mu(t)) \Phi_v'^T \mathbf{B} (\mathbf{y}(t) - \Phi_0 \mu(t)), \quad (26g)$$

$$p = T \cdot \text{tr} \left\{ \Phi_\gamma' \Sigma \Phi_\gamma'^T \mathbf{B} \right\} + \text{tr} \left\{ U^T \Phi_\gamma'^T \mathbf{B} \Phi_\gamma' U \right\} \quad (26h)$$

$$q = T \cdot \text{tr} \left\{ \Phi_0 \Sigma \Phi_\gamma'^T \mathbf{B} \right\} - \text{tr} \left\{ (\mathbf{Y} - \Phi_0 U)^T \mathbf{B} \Phi_\gamma' U \right\}, \quad (26i)$$

and $U = [\mu(1), \dots, \mu(T)]$. In (25b), δ_u , δ_v and δ_u are bounded for the fact that the first-order approximation is only valid in the vicinity of the expansion point. For simplicity expression, the detailed derivations of (24) and (25) are presented in Appendix C and Appendix D, respectively.

Denote by $f(\delta)$ the goal function in (25a), which is convex and can be globally minimized using a variety of standard optimization packages. we provide here an analytical solution for problem (25) as follows. First, we have the partial derivative with respect to δ_u as

$$\frac{\partial f}{\partial \delta_u} = 2 (M_{uu} \delta_u + M_{uv} \delta_v + \delta_\gamma v_{u\gamma} + v_u). \quad (27)$$

Thus, the minimum is achieved at $\delta_u^* = -M_{uu}^{-1} (M_{uv} \delta_v + \delta_\gamma v_{u\gamma} + v_u)$ if M_{uu} is invertible and $\delta_u^* \in [LB_u, UB_u]$. Then, we have $\delta_u^{l+1} = \delta_u^*$. Otherwise, we update δ_u element by element. Fix other elements but $(\delta_u)_i$, denote by $(\delta_u)_{-i}$ the vector δ_u without the i -th entry $(\delta_u)_i$, and then the solution to the i -th stationary point equation of $(M_{uu}^i)_{-i} (\delta_u)_{-i} + (M_{uu})_{ii} (\delta_u)_i + (M_{uv} \delta_v + \delta_\gamma v_{u\gamma} + v_u)_i = 0$ is

$$(\tilde{\delta}_u)_i = - \frac{(M_{uu}^i)_{-i} (\delta_u)_{-i} + (M_{uv} \delta_v + \delta_\gamma v_{u\gamma} + v_u)_i}{(M_{uu})_{ii}}. \quad (28)$$

Therefore, the elementwise update of δ_u^{l+1} is

$$(\delta_u^{l+1})_i = \begin{cases} (LB_u)_i, & \text{if } (\tilde{\delta}_u)_i < (LB_u)_i; \\ (\tilde{\delta}_u)_i, & \text{if } (\tilde{\delta}_u)_i \in [(LB_u)_i, (UB_u)_i]; \\ (UB_u)_i, & \text{otherwise.} \end{cases} \quad (29)$$

Following the same steps, we have the update rule for δ_v as $\delta_v^{l+1} = \delta_v^* = -M_{vv}^{-1} (M_{uv}^T \delta_u + \delta_\gamma v_{v\gamma} + v_v)$ if M_{vv} is invertible and $\delta_v^* \in [LB_v, UB_v]$. Otherwise, we have elementwise update as

$$(\delta_v^{l+1})_i = \begin{cases} (LB_v)_i, & \text{if } (\tilde{\delta}_v)_i < (LB_v)_i; \\ (\tilde{\delta}_v)_i, & \text{if } (\tilde{\delta}_v)_i \in [(LB_v)_i, (UB_v)_i]; \\ (UB_v)_i, & \text{otherwise.} \end{cases} \quad (30)$$

with

$$(\tilde{\delta}_v)_i = - \frac{(M_{vv}^i)_{-i} (\delta_v)_{-i} + (M_{uv}^T \delta_u + \delta_\gamma v_{v\gamma} + v_v)_i}{(M_{vv})_{ii}}. \quad (31)$$

In particular, minimizing problem (25) with respect to δ_γ degenerates to a scalar quadratic function optimization problem

$$\arg \min_{\delta_\gamma \in [LB_\gamma, UB_\gamma]} \left\{ p\delta_\gamma^2 + 2 \left(v_{u\gamma}^T \delta_u + v_{v\gamma}^T \delta_v + q \right) \delta_\gamma \right\}. \quad (32)$$

Note that $p > 0$, hence its minimum can be achieved either at the boundary (LB_γ or UB_γ) or at the axis of symmetry

$$\delta_\gamma^* = -\frac{v_{u\gamma}^T \delta_u + v_{v\gamma}^T \delta_v + q}{p}. \quad (33)$$

C. The Proposed PSBDL Algorithm

Based on the above analysis, the proposed parametric sparse Bayesian dictionary learning (PSBDL) algorithm is summarized in Algorithm 1. According to the outputs of Algorithm 1, we retrieve the source locations, the transmitted powers as follows.

1) *Source locations and transmitted powers estimation:* As in traditional CS-based approaches, we can estimate the spatial power spectrum of the sources with $\hat{\mathbf{X}}$ and $\hat{\mathbf{G}}$. Recall the probabilistic modeling in (11), for each row \mathbf{X}^i in the posterior estimation of \mathbf{X} , we have $\mathbf{X}^i \sim \mathcal{N}(\mathbf{U}^i, \Sigma_{ii} \mathbf{I})$. Thus, the expectation of the spatial power spectrum strength at GP $\hat{\mathbf{g}}_i$ is

$$\hat{P}_i = E \left\{ \frac{\mathbf{X}^i \mathbf{1}_T}{T} \right\} = \frac{\mathbf{U}^i \mathbf{1}_T}{T} = \frac{\hat{\mathbf{X}}^i \mathbf{1}_T}{T}, \text{ for } i = 1, \dots, N. \quad (34)$$

Then, the source locations are estimated by the GPs with the highest K peaks of the spatial power spectrum, the transmitted powers are estimated with the expected spatial power spectrum strength of the corresponding GPs.

2) *Implementation details and computational complexity:* First, N is artificially decided candidate grid point number, which is prone to be a large number greater than M . Thus, the matrix inversion operation for calculating $\Sigma \in \mathbb{R}^{N \times N}$ in Step (7) is complex and time-consuming. To this end, Woodbury matrix identity is used, when $N > M$, to reduce the dimension of the matrix inversion from N to M

$$\Sigma = \mathbf{A} - \mathbf{A} \Phi^T \Xi^{-1} \Phi \mathbf{A} \quad (35)$$

where $\Xi = \mathbf{B}^{-1} + \Phi \mathbf{A} \Phi^T$. As such, the matrix inversion computation complexity is reduced from $\mathcal{O}(N^3)$ to $\mathcal{O}(M^3)$ since $\Xi \in \mathbb{R}^{M \times M}$.

Furthermore, the dictionary approximation in Step (6) and reconstruction in Step (4) can be constrained to these grid points where the rows of \mathbf{X} are non-zero. In the proposed probabilistic model, these non-zero rows are characterized by greater variance α_i . As a result, we infer δ_u and δ_v of the GPs with the highest K variances. In this way, the coefficient matrix and coefficient vector in the goal function $f(\delta)$ can be truncated into dimension $K \times K$ or $K \times 1$, which is crucial to reduce the LLSQ problem dimension from $N + 1$ to $K + 1$ and thus to speed up the algorithm.

Based on the above implementation details, the computational complexities per iteration for the main steps are: $\mathcal{O}(KM)$ for Step (4); $\mathcal{O}(MK^2)$ for Step (6); $\mathcal{O}(MN^2 + M^2N + M^3)$ for computing Σ and $\mathcal{O}(TMN^2)$ for computing \mathbf{U} in Step (7); $\mathcal{O}(N)$ for Step (9). Generally we have $K < M < N$, thus the asymptotic complexity per iteration for the proposed PSBDL algorithm is $\mathcal{O}(TMN^2)$.

Algorithm 1: Parametric Sparse Bayesian Dictionary Learning

Input: \mathbf{Y} , K , N , \mathcal{S} , propagation model $f(\mathbf{s}_i, \mathbf{t}_k, \gamma)$.
Output: $\hat{\mathbf{X}}$, $\hat{\mathbf{G}}$ and $\hat{\gamma}$;

- 1 Initialize $\mathcal{G} = \mathcal{G}^{(0)}$, $\gamma = \gamma^{(0)}$, α , β , λ , a , b , $k = 0$;
- 2 **while** external loop stopping condition not hold **do**
- 3 $\delta_u^0 = \mathbf{0}$, $\delta_v^0 = \mathbf{0}$, $\delta_\gamma^0 = 0$, $l = 0$;
- 4 // Dictionary update
- 5 Calculate Φ_0 , Φ'_u , Φ'_v , Φ'_γ using $\mathcal{G}^{(k)}$ and $\gamma^{(k)}$;
- 6 **while** internal loop stopping condition not hold **do**
- 7 // Sparse recovery and dictionary approximation
- 8 Update Φ by (9c) using $\delta_u^{(l)}$, $\delta_v^{(l)}$, $\delta_\gamma^{(l)}$;
- 9 Compute Σ and \mathbf{U} using α^l , β^l and Φ ;
- 10 Update α^{l+1} , β^{l+1} according to (23), (22);
- 11 Calculate $\delta_u^{(l+1)}$, $\delta_v^{(l+1)}$, $\delta_\gamma^{(l+1)}$ by solving (25);
- 12 $l = l + 1$; //Update internal loop iteration counter
- 13 $\mathcal{G}^{(k+1)} = \mathcal{G}^{(k)} + \delta_g^{(l)}$, $\gamma^{(k+1)} = \gamma^{(k)} + \delta_\gamma^{(l)}$;
- 14 $k = k + 1$; //Update external loop iteration counter
- 15 **return** $\hat{\mathbf{X}} = \mathbf{U}$, $\hat{\mathbf{G}} = \mathcal{G}$, $\hat{\gamma} = \gamma$;

IV. CRAMÉR-RAO BOUND ANALYSIS

In this section, we derive the Cramér-Rao lower bound (CRLB) as an estimation benchmark for the unknown parameter vector $\vartheta = [u_1^t, v_1^t, P_1, \dots, u_K^t, v_K^t, P_K, \gamma, \beta_1, \dots, \beta_M]^T$. In estimation theory, the CRLB provides a theoretical performance limit for any unbiased estimator of the source locations $[u_k^t, v_k^t]$, the transmitted powers P_k for $k = 1, \dots, K$, as well as the PLE γ in the presence of unknown nonuniform Gaussian noise variance β_1, \dots, β_M , given the observation \mathbf{Y} .

Indeed, the CRLB gives a lower bound for the error covariance matrix

$$\mathbf{E} \left\{ (\hat{\vartheta} - \vartheta)(\hat{\vartheta} - \vartheta)^T \right\} \geq \mathbf{J}^{-1}, \quad (36)$$

where the inequality sign is defined in the positive-semidefinite (PSD) sense. $\mathbf{J} \in \mathbb{R}^{(3K+M+1) \times (3K+M+1)}$ is the Fisher information matrix (FIM) defined as

$$\mathbf{J} = \mathbf{E} \left\{ -\Delta_{\vartheta}^2 \ln p(\mathbf{Y}; \vartheta) \right\} \quad (37)$$

with $\Delta_{\vartheta}^2 = \nabla_{\vartheta} \nabla_{\vartheta}^T$ being the second derivative (Hessian) operator, and ∇_{ϑ} being the gradient operator with respect to ϑ .

Using the Gaussian observation model in and considering the MMV case, we have

$$\mathbf{J} = \sum_{t=1}^T \underbrace{\mathbf{E} \left\{ -\Delta_{\vartheta}^2 \ln p(\mathbf{y}(t); \vartheta) \right\}}_{\mathbf{J}_t}. \quad (38)$$

with $\mathbf{J}_t \in \mathbb{R}^{(3K+M+1) \times (3K+M+1)}$ being the FIM of the snapshot measurement $\mathbf{y}(t)$. The PDF of each $\mathbf{y}(t)$ is

$$p(\mathbf{y}(t); \vartheta) = \mathcal{N}(\mathbf{y}(t) | \tilde{\mu}, \mathbf{B}^{-1}) \quad (39)$$

with $\tilde{\mu}_i = \sum_{k=1}^K P_k f(\mathbf{s}_i, \mathbf{t}_k, \gamma)$, for $i = 1, \dots, M$ and $\mathbf{B} = \text{diag}(\beta_1, \dots, \beta_M)$. For the Gaussian observation vector $\mathbf{y}(t)$, the (i, j) -th element of the FIM \mathbf{J}_t can be computed as [49, Ch. 3]

$$[\mathbf{J}_t]_{i,j} = \frac{\partial \tilde{\mu}^T}{\partial \vartheta_i} \mathbf{B} \frac{\partial \tilde{\mu}}{\partial \vartheta_j} + \frac{1}{2} \text{tr} \left(\mathbf{B} \frac{\partial \mathbf{B}^{-1}}{\partial \vartheta_i} \mathbf{B} \frac{\partial \mathbf{B}^{-1}}{\partial \vartheta_j} \right) \quad (40)$$

with

$$\frac{\partial \tilde{\boldsymbol{\mu}}}{\partial \boldsymbol{\theta}_i} = \left[\frac{\partial \tilde{\mu}_1}{\partial \boldsymbol{\theta}_i}, \dots, \frac{\partial \tilde{\mu}_M}{\partial \boldsymbol{\theta}_i} \right]^T, \quad (41a)$$

$$\frac{\partial \mathbf{B}^{-1}}{\partial \boldsymbol{\theta}_i} = \text{diag} \left(\frac{\partial \beta_1^{-1}}{\partial \boldsymbol{\theta}_i}, \dots, \frac{\partial \beta_M^{-1}}{\partial \boldsymbol{\theta}_i} \right). \quad (41b)$$

For example, if the path loss model is $f(s_i, t_k, \gamma) = (d_{ik})^{-\gamma}$ with $d_{ik} = \|s_i - t_k\|_2$, then for $k = 1, \dots, K$ and $i, j = 1, \dots, M$, the non-zero partial derivative terms in (41) are

$$\frac{\partial \tilde{\mu}_i}{\partial u_k^t} = P_k \frac{\partial f(s_i, t_k, \gamma)}{\partial u_k^t} = -\gamma P_k \frac{u_k^t - u_i^s}{d_{ik}^{\gamma+2}}, \quad (42a)$$

$$\frac{\partial \tilde{\mu}_i}{\partial v_k^t} = P_k \frac{\partial f(s_i, t_k, \gamma)}{\partial v_k^t} = -\gamma P_k \frac{v_k^t - v_i^s}{d_{ik}^{\gamma+2}}, \quad (42b)$$

$$\frac{\partial \tilde{\mu}_i}{\partial P_k} = f(s_i, t_k, \gamma) = \frac{1}{d_{ik}^\gamma}. \quad (42c)$$

$$\frac{\partial \tilde{\mu}_i}{\partial \gamma} = \frac{\partial \sum_{k=1}^K P_k f(s_i, t_k, \gamma)}{\partial v_k^t} = -\sum_{k=1}^K P_k \frac{\ln d_{ik}}{d_{ik}^\gamma}, \quad (42d)$$

$$\frac{\partial \beta_j^{-1}}{\partial \beta_j} = -\frac{1}{\beta_j^2}. \quad (42e)$$

Generally, we tend to express the powers in decibels $P_{k\text{dB}} = 10 \lg P_k$, thus the partial derivative with respect to powers in decibels is

$$\frac{\partial \tilde{\mu}_i}{\partial P_{k\text{dB}}} = \frac{\partial \tilde{\mu}_i}{\partial P_k} \frac{\partial P_k}{\partial P_{k\text{dB}}} = \frac{P_k \ln 10}{10 d_{ik}^\gamma}. \quad (43)$$

V. NUMERICAL SIMULATIONS

In this section, we evaluate the localization performance of the proposed method by numerical simulations. The simulation setup refers to [39] where a square localization area of 20 m by 20 m is considered, and the path loss model is set to $f(s_i, t_k, \gamma)[\text{dB}] = -10\gamma \lg \|s_i - t_k\|_2$ when $\|s_i - t_k\|_2 > 1\text{m}$, and $f(s_i, t_k, \gamma)[\text{dB}] = 0$ otherwise. Like [39], the path-loss exponent γ is randomly drawn from [2,6], and the transmitted powers are randomly drawn from [-10 dBm, 0 dBm] in each trail. Different from [39] where only one source is considered and the sensors' locations are fixed in each trail, we deploy three sources at [5, 9], [11,17] and [15, 5], all in meters and randomly deploy the sensors inside the area in each trail to avoid sticking to any specific sensor network topology. The simulation results are averaged over $N_s = 500$ randomized trials carried out in Matlab R2016a on a PC with Windows 10 OS and an Intel i7-6700 CPU.

In the simulation, the nonuniform noise is modeled as $\varepsilon_i(t) \sim \mathcal{N}(0, \sigma_i^2)$ with $\sigma_1 \neq \sigma_2 \neq \dots \neq \sigma_M$, for which we define the signal-to-noise ratio (SNR) of the i -th sensor as $10 \lg \left(\frac{\|(\Phi(\mathcal{T}, \gamma)\mathbf{W})^i\|_2^2}{(T\sigma_i^2)} \right)$. The evaluation metric is the root-mean-square error (RMSE) defined as

$$\text{RMSE} = \sqrt{\frac{1}{K} \sum_{k=1}^K \|\boldsymbol{\theta}_k - \hat{\boldsymbol{\theta}}_k\|_2^2} \quad (44)$$

with $\hat{\boldsymbol{\theta}}_k$ being the k -th estimated parameter of truth $\boldsymbol{\theta}_k$, where $\boldsymbol{\theta}_k$ denotes t_k for source locations estimation, P_k for source

TABLE I
RMSE OF PLE ESTIMATE VERSUS THE GRID GRANULARITY

Grid granularity	6	8	10	12	14
CRLB	0.0046	0.0045	0.0045	0.0045	0.0046
PSBDL	0.1211	0.0814	0.0662	0.0661	0.0661

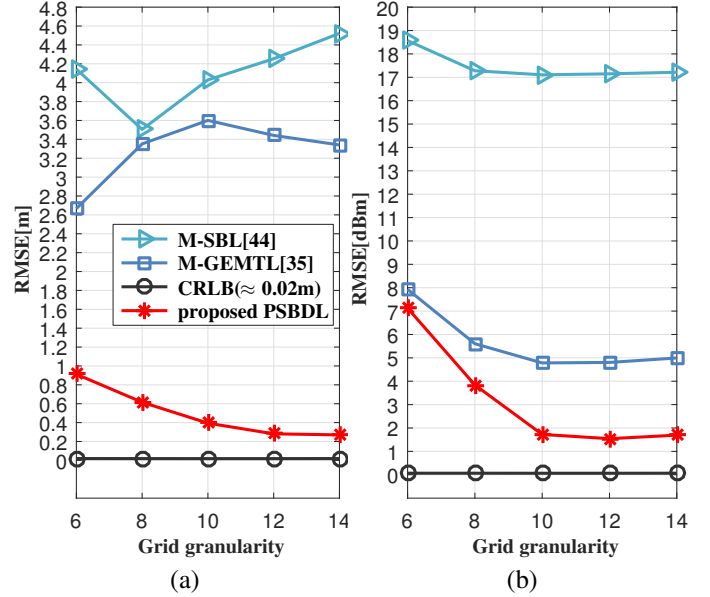


Fig. 1. The RMSE of different approaches versus the grid granularity for (a) the locations estimate and (b) the transmitted powers estimate.

powers estimation, and γ for path-loss exponent estimation with $K = 1$, respectively.

To investigate the effectiveness of the proposed approach, we compare with the traditional sparsity-based MSL algorithm M-SBL [44], the state-of-the-art off-grid MSL algorithm GEMTL [35], as well as the theoretical limits CRLB derived in Section IV. Both M-SBL and GEMTL assume the measurement noise to be uniform, and specifically, M-SBL uses the initialized parameters to form a fixed localization dictionary, while GEMTL partly infers the localization dictionary by modeling the off-grid offsets. Note that the original GEMTL algorithm is designed for SMV case, hence in the simulation, we extend it to the MMV case and term it as M-GEMTL. The path-loss exponent γ is initialized as 2 for all algorithms, and the set of candidate GPs is initialized with a uniform grid points. We examine the performance from different aspects shown as follows.

A. Impacts of Different Grid Granularity

First of all, since the number of GPs is an artificially decided parameter which may affect the estimation performance, in this simulation, we set $\text{SNR} = 25\text{dB}$, $M = 60$, and $T = 5$ to study the impacts of the grid granularity defined as \sqrt{N} with N being the number of candidate GPs. It is worth noting that the CRLB is constant for all granularity since it is irrelative to the grid discretization.

Tab. I presents the RMSE of the PLE estimate for the proposed method when the grid granularity changed from 6 to 14. It is observed that as the grid granularity increases, the RMSE of the proposed PSBDL algorithm reduces from 0.1211

TABLE II
RMSE OF PLE ESTIMATE VERSUS SNR (UNKNOWN NONUNIFORM CASE)

SNR[dB]	0	2	4	6	8	10
CRLB	0.2416	0.1869	0.1465	0.1217	0.0885	0.0380
PSBDL	0.5711	0.3983	0.2568	0.1924	0.1258	0.0926

to 0.0061 and gradually approaches the CRLB. Specifically, when the grid granularity is less than 10, as the grid granularity increases the RMSE decreases, which is because the finer grid granularity, the higher possibility to capture the off-grid sources, the higher possibility to alleviate the dictionary mismatch, and the higher accuracy of the PLE estimates. When the grid granularity is greater than 10, the RMSE of PLE almost remains constant, which is because the granularity of 10 is enough for the proposed method to capture the off-grid sources, thus the grid granularity is no longer a major influencing factor.

Fig. 1 illustrates the RMSE of the locations and transmitted powers estimates for different approaches when grid granularity changes. As expected, benefiting from the inference of the propagation parameters and the proper candidate GPs, the proposed method exhibits the lowest estimation errors, and its RMSE decreases as the grid granularity increases and is very close to the CRLB. Similar to Tab. I, when the grid granularity greater than 12, the RMSE of location estimation and transmitted powers tend to be converged. In contrast, for M-SBL and M-GEMTL, though more candidate GPs used, the RMSE of estimated locations even become larger and show no convergence, which is because the both of them have no ability to eliminate the dictionary mismatch caused by the unknown PLE. It is also shown that although the performance of M-GEMTL is inferior to the proposed method, it is still better than M-SBL, which can be explained by its capability to infer the proper candidate GPs \mathcal{G} , and thus to a certain degree it can alleviate the dictionary mismatch caused by the mismatched initial candidate GPs.

This simulation suggests that the common thought that finer candidate grid leads to higher localization accuracy may not hold for all the sparsity-based MSL methods especially in the presence of uncertain propagation parameters, unknown nonuniform noise, and off-grid sources. It is also demonstrated that owing to the inference of the unknown propagation parameters, the proposed method can effectively take advantage of the finer grid granularity and thus show better performance.

B. Impacts of Measurement Perturbation

Secondly, as it is important to investigate the MSL methods under different measurement perturbation level, in this simulation, we set $N = 121$, $M = 60$, $T = 5$, and consider the unknown nonuniform noise case. Besides, since the mean of RMSE is susceptible to outliers, and may exaggerate the estimation error, box-plot is further provided henceforth for the proposed method to display the dispersion degree, the skewness, and the outliers of its estimation errors.

Tab.II shows the RMSE of PLE estimate for the proposed method when SNR varies from 0dB to 10dB. As can be observed, the RMSE for PLE estimate of the proposed method decreases and gradually approach the theoretical CRLB when

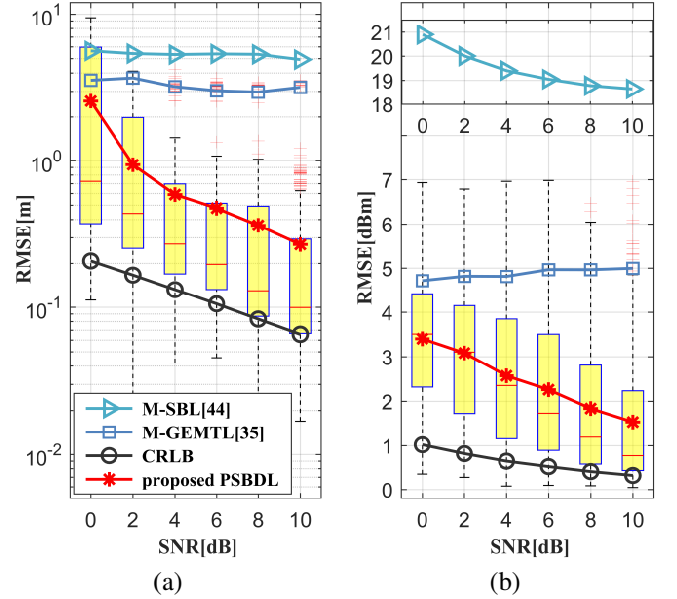


Fig. 2. The RMSE of different approaches versus SNR in the unknown nonuniform noise case for (a) the locations estimate and (b) the transmitted powers estimate.

SNR increases, which verifies the effectiveness of the proposed method to retrieve PLE information from the observations under different noise levels.

Fig.2 presents the RMSE of the locations and the transmitted powers estimations for different approaches. It is clear in Fig.2 that the proposed method is superior to other approaches and its RMSE is close to the CRLB, which can be attributed to the joint inference of PLE and the proper candidate GPs \mathcal{G} . Specifically, the RMSE of M-SBL and M-GEMTL slightly decreases as SNR increases from 0dB to 10dB, whereas for the proposed method, its RMSE significantly decreases and show the same trend as the CRLB. Moreover, the box-plot discloses more information about the estimation errors. In Fig.2(a), the second quartile or the median (red bar inside the box) is much more close to the first quartile (lower bound of the box) than the third quartile (upper bound), and the average RMSE is near the third quartile, which means the RMSE for location estimate is skewed-left and is below the average RMSE in about 75% trails. Similarly, we can see from Fig.2(b) that the RMSE of the proposed method for transmitted powers estimate is also skewed-left and more than half the trails have estimation error lower than the average RMSE.

This simulation underlines the effectiveness of the proposed method to joint learn the localization dictionary parameters and the sparse representation under different noise levels, which can greatly improve the localization performance and the robustness against the measurement perturbation.

C. Effects of the Number of Sensors and Time Snapshots

Finally, a natural method to improve the localization accuracy is to obtain more observations, i.e., to deploy more sensors and to gather more snapshot measurements. In this simulation, we study the effects of different numbers of sensors and time snapshots.

Fig.3 presents the RMSE of the locations and transmitted powers estimates for different approaches when SNR = 25dB,

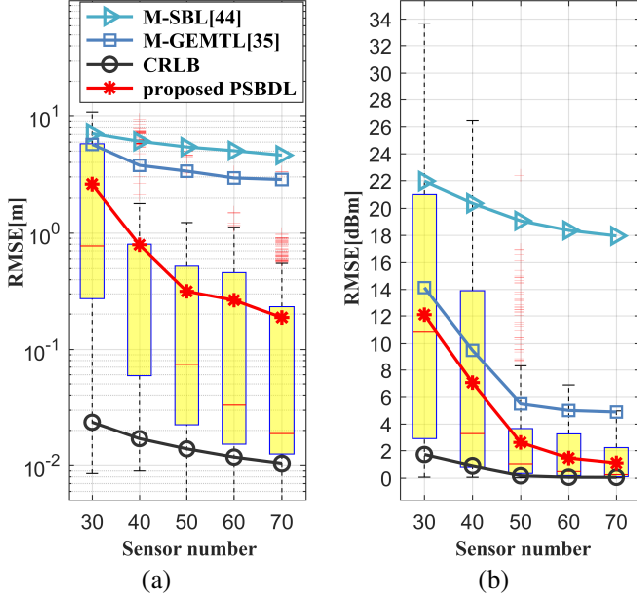


Fig. 3. The RMSE of different approaches versus the number of sensors; (a) the locations estimate and (b) the transmitted powers estimate.

$N = 121$, $T = 5$, and sensor number M varying from 30 to 70. It is observed that as the number of sensors increases, the RMSE of all algorithms decreases, which is reasonable since more information obtained, less estimate uncertainty can be achieved. Furthermore, compared with other methods, the proposed PSBDL exhibits appreciably better accuracy with the same sensor number, requires fewer sensors under the same RMSE level, and approaches the CRLB. More importantly, by comparing M-SBL, M-GEMTL, and the proposed PSBDL, we can conclude that although more sensors lead to less RMSE whether it infers the localization dictionary parameters or not, the more unknown dictionary parameters, e.g. the path-loss exponent, are effectively inferred, the more accurate estimation we obtain for the same number of sensors.

Fig.4 plots the RMSE results of the locations and transmitted powers estimates for different approaches with SNR = 25dB, $N = 121$, $M = 60$, and snapshot number T changing from 2 to 10. It is shown that the proposed method can effectively exploit the gains of more snapshots, and exhibits the best performance under all different snapshot numbers, which indicates the importance of the inference of the localization dictionary parameters and the sparse representation jointly.

Interestingly, different from Fig.3, the RMSE curve of the proposed method rapidly converges with the number of snapshots increases, and more snapshots do not significantly improve the performance of M-GEMTL, which suggests that 1) more snapshots will improve the localization accuracy but with limited ability compared with more sensors, and 2) the algorithm should be carefully designed to effectively utilize the information gains of more snapshot data.

This simulation indicates that the proposed method can effectively exploit the gains of more sensors and more snapshots which will contribute to the improvement of estimation accuracy.

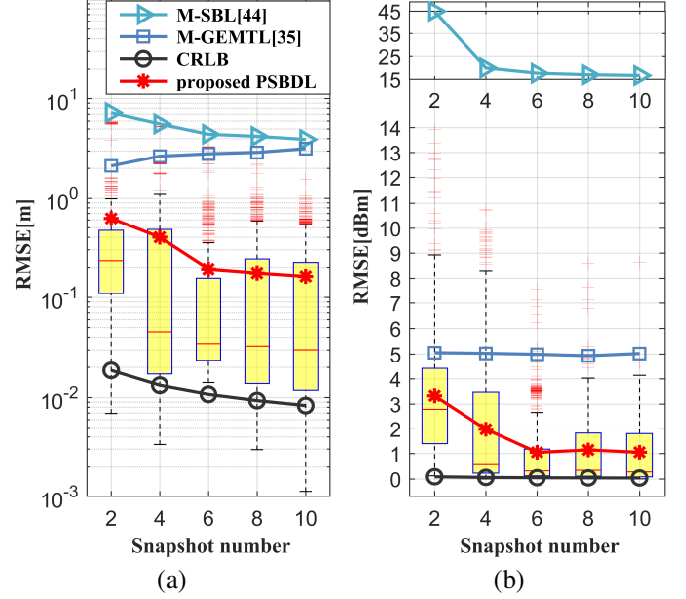


Fig. 4. The RMSE of different approaches versus the number of snapshots; (a) the locations estimate and (b) the transmitted powers estimate.

VI. DISCUSSION

In this section, we first provide a Bayesian gain interpretation to further understand the proposed algorithm, and then clarify its difference with some well-known dictionary learning algorithms.

A. Bayesian Gain Interpretation for the Proposed Algorithm

To further understand the mechanism of the proposed algorithm, we illustrate by Fig. 5 the Bayesian gains under different treatments from the perspective of Bayesian inference. The logarithmic marginal likelihood $\ln p(Y, \alpha, \beta; \mathcal{G}, \gamma)$ serves as not only the goal function, but also the measurement of matching degree among the observation, the probabilistic model inference, and the localization dictionary.

Note that for all treatments in Fig. 5, both the true grid $\bar{\mathcal{G}}$ and the true PLE $\bar{\gamma}$ is unknown, and the initial values $\mathcal{G}^{(0)}$ and $\gamma^{(0)}$ differ from the truth. It is obvious that inferring \mathcal{G} and γ jointly (the proposed treatment) brings much higher likelihood than only inferring \mathcal{G} (state-of-the-art off-grid MSL treatment, e.g. [34], [35]), which can be attributed to the gain of PLE

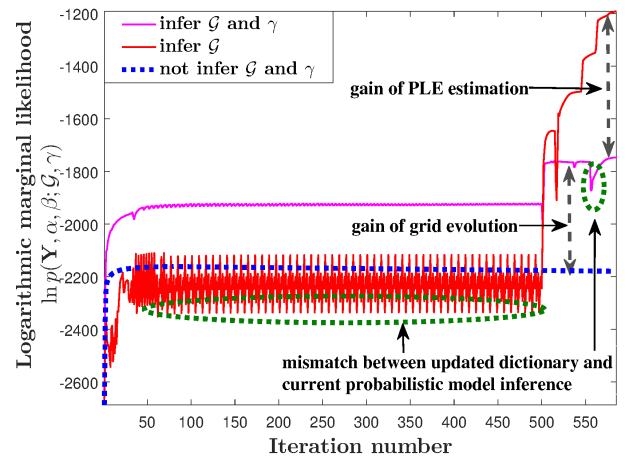


Fig. 5. Changes of the logarithmic marginal likelihood along with iterations.

estimation, while the likelihood of the latter is higher than not inferring the localization dictionary parameter \mathcal{G} and γ (conventional CS-based treatment, i.e. [29], [30], [44]), which is owing to the gain of grid evolution. More specifically, if we do not infer the localization dictionary (namely \mathcal{G} and γ), the likelihood curve, shown by the blue dotted line, exhibits the typical smooth convergence curve of EM algorithm, while the curves of all other treatment, shown by magenta and red solid lines, grow in stages. Those stages are internal iterations of the algorithms, and the likelihood may drop at the edges of those stages, owing to the mismatch between the updated dictionary model and current probabilistic inference.

B. Difference with Some Dictionary Learning Problems

Problem (7) may have other interpretations such as underdetermined blind source separation [50] and other CS dictionary learning problems, such as K-SVD [51]. The difference is that in these works, the coefficient matrix or dictionary matrix Φ need not have a certain physical structure and the only requirement is that \mathbf{Y} has sparse representation under Φ , while for the localization problem here, Φ are physical structured, or more precisely, parameterized by the dictionary parameters of interest according to a certain physical model.

Mathematically, the original MSL problem shown in Section II-A is a highly nonlinear and nonconvex continuous multi-parameter optimization problem, which is hard to solve directly. In this paper, like piecewise linear approximation, we use a series of discrete parametric dictionary model to iteratively approximate the original complex continuous optimization problem, and reformulate the original problem as a sparse recovery problem under the parametric discrete dictionary. In each iteration, we jointly infer the optimal step of current dictionary parameters to the truth and the sparse representation under current dictionary, which is implemented by the incorporation of dictionary approximation model and sparse Bayesian learning framework. Hence, we termed the proposed method as parametric sparse Bayesian dictionary learning.

VII. CONCLUSION

In this paper, we have investigated the multiple co-channel sources localization problem based on RSS measurements in the presence of unknown nonuniform measurement perturbations and uncertain propagation parameters including both the transmitted powers and the path-loss exponent. The original MSL problem is highly nonconvex and hard to solve. With the combination of the sparsity-based MSL model and the localization dictionary approximation model, we have reformulated the original MSL problem into a joint PSDL and SSR problem which was solved by the proposed PSDBL method. Extensive simulations were carried out compared with the state-of-the-art sparsity-based MSL methods and the theoretical CRLB we derived. Numerical results highlighted the effectiveness and superiority of the proposed method, and also shed light on its importance and feasibility of jointly inferring from the RSS measurements the source locations and the propagation parameters. Mathematically, this paper

provides a paradigm to enforce sparse representation and approximate a continuous sparsifying parametric dictionary by a series of discrete parametric dictionary simultaneously.

APPENDIX A DERIVATION OF (22)

To obtain Eq. (22), first let $Q(\alpha) = E \{ \ln p(\mathbf{X}|\alpha)p(\alpha) \}$. Then we have

$$\begin{aligned} Q(\alpha) &= E \left\{ -\frac{1}{2} \sum_{t=1}^T \left(\ln |\mathbf{A}| + \mathbf{x}(t)^T \mathbf{A}^{-1} \mathbf{x}(t) \right) + \sum_{i=1}^N \left(\ln \lambda - \frac{\lambda}{2} \alpha_i \right) \right\} \\ &\quad + \text{const} \\ &= -\frac{1}{2} \sum_{t=1}^T \left\{ \sum_{i=1}^N \ln \alpha_i + \sum_{i=1}^N \alpha_i^{-1} \left(\mu(t)_i^2 + \Sigma_{ii} \right) \right\} \\ &\quad + \sum_{i=1}^N \left(\ln \lambda - \frac{\lambda}{2} \alpha_i \right) + \text{const} \end{aligned} \quad (45)$$

with const being the item constant to α . To find the stationary point of $Q(\alpha)$ w.r.t α_i , let $\partial Q(\alpha)/\partial \alpha_i = 0$, and then we obtain

$$\alpha_i = \frac{\sqrt{T^2 + 4\lambda \sum_{t=1}^T (\Sigma_{ii} + \mu(t)_i^2)} - T}{2\lambda}. \quad (46)$$

APPENDIX B DERIVATION OF (23)

Let $Q(\beta) = E \{ p(\mathbf{Y}|\mathbf{X}, \beta, \gamma; \mathcal{G})p(\beta) \}$. Then, we have

$$\begin{aligned} Q(\beta) &= E \left\{ \frac{1}{2} \sum_{t=1}^T \left(\ln |\mathbf{B}| - (\mathbf{y}(t) - \Phi \mathbf{x}(t))^T \mathbf{B} (\mathbf{y}(t) - \Phi \mathbf{x}(t)) \right) \right. \\ &\quad \left. + \sum_{j=1}^M ((a-1) \ln \beta_j - b \beta_j) \right\} + \text{const} \\ &= \frac{1}{2} \sum_{t=1}^T \left(\ln |\mathbf{B}| - \sum_{j=1}^M \beta_j E \left\{ (\mathbf{y}(t) - \Phi \mathbf{x}(t))_j^2 \right\} \right) \\ &\quad + (a-1) \ln |\mathbf{B}| - b \sum_{j=1}^M \beta_j + \text{const} \\ &= \left(a-1 + \frac{T}{2} \right) \sum_{j=1}^M \ln \beta_j \\ &\quad - \frac{1}{2} \sum_{j=1}^M \beta_j \sum_{t=1}^T E \left\{ (\mathbf{y}(t) - \Phi \mathbf{x}(t))_j^2 \right\} - b \sum_{j=1}^M \beta_j + \text{const} \end{aligned} \quad (47)$$

where const is the item constant to β . let $\partial Q(\beta)/\partial \beta_j = 0$, we have

$$\beta_j = \frac{2a-2+T}{2b + \sum_{t=1}^T E \left\{ (\mathbf{y}(t) - \Phi \mathbf{x}(t))_j^2 \right\}} \quad (48)$$

Since $\mathbf{y}(t) - \Phi\mathbf{x}(t) \sim \mathcal{N}(\mathbf{y}(t) - \Phi\boldsymbol{\mu}(t), \Phi\Sigma\Phi^T)$, denote by \mathbf{e}_j the unit column vector with its j -th element being one, then we have

$$\begin{aligned} & E \left\{ (\mathbf{y}(t) - \Phi\mathbf{x}(t))_j^2 \right\} \\ &= E \left\{ (\mathbf{y}(t) - \Phi\mathbf{x}(t))^T \mathbf{e}_j \mathbf{e}_j^T (\mathbf{y}(t) - \Phi\mathbf{x}(t)) \right\} \\ &= \text{tr} \left(\mathbf{e}_j \mathbf{e}_j^T \Phi \Sigma \Phi^T \right) + (\mathbf{y}(t) - \Phi\boldsymbol{\mu}(t))^T \mathbf{e}_j \mathbf{e}_j^T (\mathbf{y}(t) - \Phi\boldsymbol{\mu}(t)) \\ &= \text{tr} \left(\mathbf{e}_j^T \Phi \Sigma \Phi^T \mathbf{e}_j \right) + (\mathbf{y}(t) - \Phi\boldsymbol{\mu}(t))_j^2 \\ &= \left(\Phi \Sigma \Phi^T \right)_{jj} + (\mathbf{y}(t) - \Phi\boldsymbol{\mu}(t))_j^2. \end{aligned} \quad (49)$$

Finally, substituting (49) into Eq.(48), we obtain the update formula shown by Eq.(23).

APPENDIX C DERIVATION OF (24)

Eq.(24) is based on the following properties: if $\mathbf{x} \sim \mathcal{N}(\boldsymbol{\mu}, \Sigma)$, then we have

$$E \{ \mathbf{x}^T \mathbf{A} \mathbf{x} \} = \boldsymbol{\mu}^T \mathbf{A} \boldsymbol{\mu} + \text{tr}(\mathbf{A} \Sigma). \quad (50)$$

With this property, we obtain Eq.(24) as

$$\begin{aligned} & E \left\{ \sum_{t=1}^T (\mathbf{y}(t) - \Phi\mathbf{x}(t))^T \mathbf{B} (\mathbf{y}(t) - \Phi\mathbf{x}(t)) \right\} \\ &= \sum_{t=1}^T \left\{ \mathbf{y}(t)^T \mathbf{B} \mathbf{y}(t) - 2\boldsymbol{\mu}(t)^T \Phi^T \mathbf{B} \mathbf{y}(t) + E \{ \mathbf{x}(t)^T \Phi^T \mathbf{B} \Phi \mathbf{x}(t) \} \right\} \\ &= \sum_{t=1}^T \left\{ (\mathbf{y}(t) - \Phi\boldsymbol{\mu}(t))^T \mathbf{B} (\mathbf{y}(t) - \Phi\boldsymbol{\mu}(t)) + \text{tr}(\Phi \Sigma \Phi^T \mathbf{B}) \right\}. \end{aligned} \quad (51)$$

APPENDIX D DERIVATION OF (25)

To obtain the goal function in (25a), we first introduce the following matrix identities:

$$\mathbf{v}^T \text{diag}(\mathbf{u}) = \mathbf{u}^T \text{diag}(\mathbf{v}), \quad (52)$$

$$\text{diag}(\mathbf{v}) \cdot \mathbf{M} \cdot \text{diag}(\mathbf{u}) = \mathbf{M} \circ \mathbf{v} \mathbf{u}^T, \quad (53)$$

$$\text{tr} \{ \text{diag}(\mathbf{v})^H \mathbf{Q} \text{diag}(\mathbf{u}) \mathbf{R}^T \} = \mathbf{v}^H (\mathbf{Q} \circ \mathbf{R}) \mathbf{u}, \quad (54)$$

for vector \mathbf{v} , \mathbf{u} , and matrices \mathbf{Q} and \mathbf{R} with proper dimension, where $(\cdot)^H$ denotes the conjugate transpose operator.

Then, substituting (9c) into Eq. (24), by (52) and (53) we have the first term inside the RHS of Eq. (24) expressed as

$$\begin{aligned} & (\mathbf{y}(t) - \Phi\boldsymbol{\mu}(t))^T \mathbf{B} (\mathbf{y}(t) - \Phi\boldsymbol{\mu}(t)) \\ &= \delta_\gamma^2 \left(\Phi_\gamma' \boldsymbol{\mu}(t) \right)^T \mathbf{B} \Phi_\gamma' \boldsymbol{\mu}(t) + \sum_{\chi=u,v} \delta_\chi^T \left(\Phi_\chi'^T \mathbf{B} \Phi_\chi' \circ \boldsymbol{\mu}(t) \boldsymbol{\mu}(t)^T \right) \delta_\chi \\ &+ 2\delta_u^T \left(\Phi_u'^T \mathbf{B} \Phi_u' \circ \boldsymbol{\mu}(t) \boldsymbol{\mu}(t)^T \right) \delta_u + 2\delta_\gamma \sum_{\chi=u,v} \delta_\chi^T \left(\Phi_\chi'^T \mathbf{B} \Phi_\gamma' \circ \boldsymbol{\mu}(t) \boldsymbol{\mu}(t)^T \right) \mathbf{1}_N \\ &- 2\delta_\gamma (\mathbf{y}(t) - \Phi_0 \mathbf{u}(t))^T \mathbf{B} \Phi_\gamma' \text{diag}(\mathbf{u}(t)) \\ &- 2 \sum_{\chi=u,v} (\mathbf{y}(t) - \Phi_0 \boldsymbol{\mu}(t))^T \mathbf{B} \Phi_\chi' \text{diag}(\boldsymbol{\mu}(t)) \delta_\chi + \text{const}, \end{aligned} \quad (55)$$

and by (54), we obtain the second term inside the RHS of Eq. (24) as

$$\begin{aligned} & \text{tr} \left\{ \left(\Phi_0 + \Phi_u' \Delta_u + \Phi_v' \Delta_v + \delta_\gamma \Phi_\gamma' \right) \Sigma \left(\Phi_0 + \Phi_u' \Delta_u + \Phi_v' \Delta_v + \delta_\gamma \Phi_\gamma' \right)^T \mathbf{B} \right\} \\ &= \delta_\gamma^2 \text{tr} \left\{ \Phi_\gamma' \Sigma \Phi_\gamma'^T \mathbf{B} \right\} + \sum_{\chi=u,v} \delta_\chi^T \left(\Phi_\chi'^T \mathbf{B} \Phi_\chi' \circ \Sigma \right) \delta_\chi + 2\delta_u^T \left(\Phi_u'^T \mathbf{B} \Phi_v' \circ \Sigma \right) \delta_v \\ &+ 2\delta_\gamma \sum_{\chi=u,v} \delta_\chi^T \left(\Phi_\chi'^T \mathbf{B} \Phi_\gamma' \circ \Sigma \right) \mathbf{1}_N + 2 \sum_{\chi=u,v} \text{diag} \left(\Phi_\chi' \mathbf{B} \Phi_0 \Sigma \right)^T \delta_\chi \\ &+ 2\delta_\gamma \text{tr} \left\{ \Phi_0 \Sigma \Phi_\gamma'^T \mathbf{B} \right\} + \text{const} \end{aligned} \quad (56)$$

where const is constant independent of δ_u , δ_v and δ_γ . Finally, by plugging these terms into (24), we obtain the goal function in (25).

REFERENCES

- [1] R. Niu, A. Vempaty, and P. K. Varshney, "Received-signal-strength-based localization in wireless sensor networks," *Proc. IEEE*, vol. 106, no. 7, pp. 1166–1182, July 2018.
- [2] M. Z. Win, A. Conti, S. Mazuelas, Y. Shen, W. M. Gifford, D. Dardari, and M. Chiani, "Network localization and navigation via cooperation," *IEEE Commun. Mag.*, vol. 49, no. 5, pp. 56–62, May 2011.
- [3] D. Lymberopoulos and J. Liu, "The microsoft indoor localization competition: Experiences and lessons learned," *IEEE Signal Processing Mag.*, vol. 34, no. 5, pp. 125–140, Sept 2017.
- [4] K. W. Cheung, H. C. So, W. K. Ma, and Y. T. Chan, "Least squares algorithms for time-of-arrival-based mobile location," *IEEE Trans. Signal Processing*, vol. 52, no. 4, pp. 1121–1130, 2004.
- [5] Y. Wang and K. C. Ho, "Tdoa positioning irrespective of source range," *IEEE Trans. Signal Processing*, vol. 65, no. 6, pp. 1447–1460, March 2017.
- [6] X. Qu, L. Xie, and W. Tan, "Iterative constrained weighted least squares source localization using tdoa and fdoa measurements," *IEEE Trans. Signal Processing*, vol. 65, no. 15, pp. 3990–4003, Aug 2017.
- [7] L. C. Godara, "Application of antenna arrays to mobile communications. ii. beam-forming and direction-of-arrival considerations," *Proc. IEEE*, vol. 85, no. 8, pp. 1195–1245, 1997.
- [8] S. Stein, O. Yair, D. Cohen, and Y. C. Eldar, "Cascade: Compressed carrier and doa estimation," *IEEE Trans. Signal Processing*, vol. 65, no. 10, pp. 2645–2658, 2017.
- [9] T. Peng, P. Zuo, K. You, H. Jing, W. Guo, and W. Wang, "Bounds and methods for multiple directional sources localization based on rss measurements," *IEEE Access*, vol. 7, pp. 131 395–131 406, 2019.
- [10] P. Zuo, T. Peng, K. You, W. Guo, and W. Wang, "Rss-based localization of multiple directional sources with unknown transmit powers and orientations," *IEEE Access*, vol. 7, pp. 88 756–88 767, 2019.
- [11] X. Sheng and Y.-H. Hu, "Maximum likelihood multiple-source localization using acoustic energy measurements with wireless sensor networks," *IEEE Trans. Signal Processing*, vol. 53, no. 1, pp. 44–53, Jan 2005.
- [12] F. Bandiera, A. Coluccia, and G. Ricci, "A cognitive algorithm for received signal strength based localization," *IEEE Trans. Signal Processing*, vol. 63, no. 7, pp. 1726–1736, April 2015.
- [13] J. Yan, C. C. J. M. Tiberius, P. J. G. Teunissen, G. Bellusci, and G. J. M. Janssen, "A framework for low complexity least-squares localization with high accuracy," *IEEE Trans. Signal Processing*, vol. 58, no. 9, pp. 4836–4847, Sept 2010.
- [14] S. Gezici, Z. Tian, G. B. Giannakis, H. Kobayashi, A. F. Molisch, H. V. Poor, and Z. Sahinoglu, "Localization via ultra-wideband radios: a look at positioning aspects for future sensor networks," *IEEE Trans. Signal Processing*, vol. 22, no. 4, pp. 70–84, July 2005.
- [15] G. Mao, B. Fidan, and B. D. O. Anderson, "Wireless sensor network localization techniques," *Comput. Netw.*, vol. 51, no. 10, pp. 2529–2553, 2007.
- [16] T. L. T. Nguyen, F. Septier, H. Rajaona, G. W. Peters, I. Nevat, and Y. Delignon, "A bayesian perspective on multiple source localization in wireless sensor networks," *IEEE Trans. Signal Processing*, vol. 64, no. 7, pp. 1684–1699, April 2016.
- [17] D. E. Manolakis, "Efficient solution and performance analysis of 3-d position estimation by trilateration," *IEEE Trans. Aerosp. Electron. Syst.*, vol. 32, no. 4, pp. 1239–1248, Oct 1996.

- [18] S. Mazuelas, A. Bahillo, R. M. Lorenzo, P. Fernandez, F. A. Lago, E. Garcia, J. Blas, and E. J. Abril, "Robust indoor positioning provided by real-time rssi values in unmodified wlan networks," *IEEE J. Sel. Top. Sign. Proces.*, vol. 3, no. 5, pp. 821–831, Oct 2009.
- [19] N. Patwari, A. O. Hero, M. Perkins, N. S. Correal, and R. J. O'Dea, "Relative location estimation in wireless sensor networks," *IEEE Trans. Signal Processing*, vol. 51, no. 8, pp. 2137–2148, Aug 2003.
- [20] A. Coluccia and F. Ricciato, "On ml estimation for automatic rss-based indoor localization," in *Proc. IEEE Int. Symp. Wireless Pervas. Comput.*, May 2010, pp. 495–502.
- [21] D. Li and Y. H. Hu, "Energy-based collaborative source localization using acoustic microsensor array," *EURASIP J. Appl. Signal Process.*, vol. 2003, no. 4, pp. 3990–4003, Aug 2003.
- [22] H. C. So and L. Lin, "Linear least squares approach for accurate received signal strength based source localization," *IEEE Trans. Signal Processing*, vol. 59, no. 8, pp. 4035–4040, Aug 2011.
- [23] M. R. Gholami, H. Wymeersch, E. G. Strom, and M. Rydstrom, "Wireless network positioning as a convex feasibility problem," *Eurasip Journal on Wireless Communications and Networking*, vol. 2011, no. 1, p. 161, 2011.
- [24] G. Wang and K. Yang, "A new approach to sensor node localization using rss measurements in wireless sensor networks," *IEEE Trans. Wireless Commun.*, vol. 10, no. 5, pp. 1389–1395, May 2011.
- [25] M. R. Palattella, M. Dohler, A. Grieco, G. Rizzo, J. Torsner, T. Engel, and L. Ladid, "Internet of things in the 5g era: Enablers, architecture, and business models," *IEEE J. Select. Areas Commun.*, vol. 34, no. 3, pp. 510–527, March 2016.
- [26] C. Feng, S. Valaee, and Z. Tan, "Multiple target localization using compressive sensing," in *Proc. GLOBECOM*, Nov 2009, pp. 1–6.
- [27] V. Cevher, M. F. Duarte, and R. G. Baraniuk, "Distributed target localization via spatial sparsity," in *2008 16th European Signal Processing Conference*, Aug 2008, pp. 1–5.
- [28] C. Feng, W. S. A. Au, S. Valaee, and Z. Tan, "Compressive sensing based positioning using rss of wlan access points," in *Proc. IEEE INFOCOM*, March 2010, pp. 1–9.
- [29] B. Zhang, X. Cheng, N. Zhang, Y. Cui, Y. Li, and Q. Liang, "Sparse target counting and localization in sensor networks based on compressive sensing," in *Proc. IEEE INFOCOM*, April 2011, pp. 2255–2263.
- [30] C. Feng, W. S. A. Au, S. Valaee, and Z. Tan, "Received-signal-strength-based indoor positioning using compressive sensing," *IEEE Trans. Mobile Comput.*, vol. 11, no. 12, pp. 1983–1993, Dec 2012.
- [31] E. J. Candes and M. B. Wakin, "An introduction to compressive sampling," *IEEE Signal Processing Mag.*, vol. 25, no. 2, pp. 21–30, March 2008.
- [32] Y. Chi, L. L. Scharf, A. Pezeshki, and A. R. Calderbank, "Sensitivity to basis mismatch in compressed sensing," *IEEE Trans. Signal Processing*, vol. 59, no. 5, pp. 2182–2195, May 2011.
- [33] B. Sun, Y. Guo, N. Li, and D. Fang, "Multiple target counting and localization using variational Bayesian EM algorithm in wireless sensor networks," *IEEE Trans. Commun.*, vol. 65, no. 7, pp. 2985–2998, July 2017.
- [34] —, "An efficient counting and localization framework for off-grid targets in WSNs," *IEEE Commun. Lett.*, vol. 21, no. 4, pp. 809–812, April 2017.
- [35] K. You, W. Guo, Y. Liu, W. Wang, and Z. Sun, "Grid evolution: Joint dictionary learning and sparse bayesian recovery for multiple off-grid targets localization," *IEEE Commun. Lett.*, vol. 22, no. 10, pp. 2068–2071, Oct 2018.
- [36] Y. Hu and G. Leus, "Self-estimation of path-loss exponent in wireless networks and applications," *IEEE Transactions on Vehicular Technology*, vol. 64, no. 11, pp. 5091–5102, Nov 2015.
- [37] R. Sari and H. Zayyani, "RSS localization using unknown statistical path loss exponent model," *IEEE Communications Letters*, vol. 22, no. 9, pp. 1830–1833, Sept 2018.
- [38] R. M. Vaghefi, M. R. Gholami, R. M. Buehrer, and E. G. Strom, "Cooperative received signal strength-based sensor localization with unknown transmit powers," *IEEE Transactions on Signal Processing*, vol. 61, no. 6, pp. 1389–1403, March 2013.
- [39] M. R. Gholami, R. M. Vaghefi, and E. G. Strm, "Rss-based sensor localization in the presence of unknown channel parameters," *IEEE Trans. Signal Processing*, vol. 61, no. 15, pp. 3752–3759, Aug 2013.
- [40] D. P. Wipf and B. D. Rao, "An empirical bayesian strategy for solving the simultaneous sparse approximation problem," *IEEE Trans. Signal Processing*, vol. 55, no. 7, pp. 3704–3716, July 2007.
- [41] J. Chen and X. Huo, "Theoretical results on sparse representations of multiple-measurement vectors," *IEEE Transactions on Signal Processing*, vol. 54, no. 12, pp. 4634–4643, Dec 2006.
- [42] D. Malioutov, M. Cetin, and A. S. Willsky, "A sparse signal reconstruction perspective for source localization with sensor arrays," *IEEE Transactions on Signal Processing*, vol. 53, no. 8, pp. 3010–3022, Aug 2005.
- [43] S. F. Cotter, B. D. Rao, Kjersti Engan, and K. Kreutz-Delgado, "Sparse solutions to linear inverse problems with multiple measurement vectors," *IEEE Transactions on Signal Processing*, vol. 53, no. 7, pp. 2477–2488, July 2005.
- [44] D. P. Wipf and B. D. Rao, "An empirical bayesian strategy for solving the simultaneous sparse approximation problem," *IEEE Transactions on Signal Processing*, vol. 55, no. 7, pp. 3704–3716, July 2007.
- [45] S. D. Babacan, R. Molina, and A. K. Katsaggelos, "Bayesian compressive sensing using laplace priors," *IEEE Trans. Signal Processing*, vol. 19, no. 1, pp. 53–63, Jan 2010.
- [46] R. Tibshirani, "Regression shrinkage and selection via the lasso," *Journal of the Royal Statistical Society. Series B (Methodological)*, pp. 267–288, 1996.
- [47] M. E. Tipping, "Sparse bayesian learning and the relevance vector machine," *Journal of Machine Learning Research*, vol. 1, pp. 211–244, 2001.
- [48] S. Ji, Y. Xue, and L. Carin, "Bayesian compressive sensing," *IEEE Trans. Signal Processing*, vol. 56, no. 6, pp. 2346–2356, June 2008.
- [49] S. M. Kay, "Fundamentals of statistical signal processing: estimation theory," *Technometrics*, vol. 37, no. 4, p. 465, 1993.
- [50] P. Georgiev, F. Theis, and A. Cichocki, "Sparse component analysis and blind source separation of underdetermined mixtures," *IEEE Trans. Neural Networks*, vol. 16, no. 4, pp. 992–996, July 2005.
- [51] M. Aharon, M. Elad, and A. Bruckstein, "K-svd: An algorithm for designing overcomplete dictionaries for sparse representation," *IEEE Trans. Signal Processing*, vol. 54, no. 11, pp. 4311–4322, Nov 2006.